

# **Device Physics of Thin-Film Polycrystalline Cells and Modules**

## **Annual Subcontract Report 6 December 1995 - 5 December 1996**

J.R. Sites

*Department of Physics  
Colorado State University  
Fort Collins, Colorado*

NREL technical monitor: B. von Roedern



National Renewable Energy Laboratory  
1617 Cole Boulevard  
Golden, Colorado 80401-3393  
A national laboratory of  
the U.S. Department of Energy  
Managed by Midwest Research Institute  
for the U.S. Department of Energy  
under Contract No. DE-AC36-83CH10093

Prepared under Subcontract No. XAX-4-14000-01

October 1997

This publication was reproduced from the best available camera-ready copy submitted by the subcontractor and received no editorial review at NREL.

#### NOTICE

This report was prepared as an account of work sponsored by an agency of the United States government. Neither the United States government nor any agency thereof, nor any of their employees, makes any warranty, express or implied, or assumes any legal liability or responsibility for the accuracy, completeness, or usefulness of any information, apparatus, product, or process disclosed, or represents that its use would not infringe privately owned rights. Reference herein to any specific commercial product, process, or service by trade name, trademark, manufacturer, or otherwise does not necessarily constitute or imply its endorsement, recommendation, or favoring by the United States government or any agency thereof. The views and opinions of authors expressed herein do not necessarily state or reflect those of the United States government or any agency thereof.

Available to DOE and DOE contractors from:

Office of Scientific and Technical Information (OSTI)  
P.O. Box 62  
Oak Ridge, TN 37831

Prices available by calling (423) 576-8401

Available to the public from:

National Technical Information Service (NTIS)  
U.S. Department of Commerce  
5285 Port Royal Road  
Springfield, VA 22161  
(703) 487-4650



## SUMMARY

During 1996, a number of projects were carried out at Colorado State University on Cu(In,Ga)Se<sub>2</sub> (CIGS) and CdTe solar cells and small modules:

- (1) Colorado State participated directly in the deposition of CIGS at NREL for the first time. Five separate substrates were used, and sodium was both deliberately introduced and deliberately blocked from exiting soda-lime substrates. In general, sodium in the CIGS led to better junction properties and higher efficiency.
- (2) In other CIGS measurements, we showed that electrodeposited absorber material made at NREL produced competitive cells. Voltages, normalized to bandgap, were about 50 mV less than the best evaporated CIGS cells. We also showed, in collaboration with Solarex, that existence of a high resistivity ZnO layer is probably not critical for cells with relatively thick CdS window layers.
- (3) In collaboration with seven CdTe fabrication labs, we measured the effect of CdS thickness on cell parameters. Although voltage and fill-factor generally degrade for CdS thickness below 100 nm, the exceptions suggest that with at least some fabrication techniques, CdS thickness can be reduced to the point that high quantum efficiency in the blue and a good diode junction are not mutually exclusive.
- (4) A number of artifacts that appear in module measurement and analysis, but are generally negligible for small test cells, were investigated. These include effects due to module-cell geometry and misleading conclusions from selective illumination experiments.
- (5) NREL data from the highest efficiency CIGS and CdTe cells were analyzed to provide direct comparisons of different fabrication techniques. The three commonly used NREL deposition systems have produced CIGS cells with very similar junction properties. Similarly, after adjustment for bandgap, the best South Florida junctions from several years ago are remarkably similar to those produced by Golden Photon in 1996.
- (6) Colorado State continues to play a significant role in both the CIGS Thin-Film and the CdTe projects summarized above. I have served on the CIGS logistics team and have worked towards a common format for cell-data exchange between laboratories.

# TABLE OF CONTENTS

SUMMARY .....	ii
FIGURES .....	iv
INTRODUCTION .....	1
CELL DEPOSITION .....	2
CELL ANALYSIS .....	7
CIS and CIGS .....	7
CdTe .....	14
MODULE ANALYSIS .....	20
RECOMMENDATIONS .....	26
COMMUNICATIONS .....	27
Publications .....	27
Presentations .....	27
Graduate Degrees .....	27
Specific Cell/Module Reports .....	28

## FIGURES

Figure 1.	Sodium effect on CIGS I-V curves . . . . .	3
Figure 2.	Trends in basic parameters due to sodium . . . . .	4
Figure 3.	Trends in fill-factor parameters due to sodium . . . . .	5
Figure 4.	Trend in CIGS hole density with sodium . . . . .	6
Figure 5.	I-V and QE for electrodeposited CIGS cells . . . . .	8
Figure 6.	Voltage/bandgap comparison for CIGS cells . . . . .	9
Figure 7.	Impact of high-resistivity ZnO . . . . .	10
Figure 8.	Comparison of best cells from three NREL systems . . . . .	12
Figure 9.	Logarithmic comparison of Fig. 8 data . . . . .	13
Figure 10.	Variation in CdTe QE with CdS thickness . . . . .	15
Figure 11.	CdTe voltage and fill factor vs. CdS absorption . . . . .	16
Figure 12.	Comparison of high-efficiency CdTe cells . . . . .	17
Figure 13.	QE cutoffs for GPI and USF CdTe cells . . . . .	18
Figure 14.	Logarithmic comparison of Fig. 12 data . . . . .	19
Figure 15.	Module interconnect patterns . . . . .	20
Figure 16.	Schematic of large-scale laser scanner at NREL . . . . .	21
Figure 17.	Effect of a shunt on laser scan . . . . .	22
Figure 18.	Shunt and photocurrent effects of a pin prick . . . . .	22
Figure 19.	Module cell current-voltage measurement . . . . .	23
Figure 20.	Voltage-probe placement options for module cell . . . . .	24

## INTRODUCTION

The objectives of the Colorado State program are (1) the separation and quantification of individual losses in specific thin-film solar cells, (2) the detailed characterization of small modules, and (3) the presentation of a viable model for the forward-current loss mechanism. Progress was made in each of these areas.

Five research students were responsible for most of the experimental and analytical work. Ingrid Eisgruber, who completed her Ph.D. in March 1996 and now works at the Materials Research Group, did essentially all of the work on modules. Jennifer Granata has been responsible for systematic comparisons of both CdTe and CIS cells and has begun her Ph.D. thesis work on the effect of sodium in CIGS cells. Brendon Murphy and Karl Schmidt worked on smaller projects focused on specific cells, and completed their Masters' degrees during 1996. Jason Hiltner joined us Summer 1996 and has been responsible for updating much of the data collection software.

The Colorado State program continues to collaborate closely with a number of other laboratories. During the past year active collaborations have included Golden Photon, Inc., the Institute of Energy Conversion, International Solar Electric Technology, Inc., the National Renewable Energy Laboratory, Solar Cells, Inc., Siemens Solar Industries, Solarex, Energy Photovoltaics, Inc., the University of South Florida, the University of Toledo, and the Colorado School of Mines.

## CELL DEPOSITION

In a continuation of work begun by Tuttle and colleagues at NREL<sup>1</sup>, Jennifer Granata modified the sodium content in CIGS cells deposited on molybdenum/soda-lime glass from three sources, Mo/alumina, and Mo/stainless-steel.<sup>2</sup> In each case, four different sodium conditions were used. In presumed increasing order of sodium concentration; these were (a) a diffusion barrier of SiO<sub>2</sub> (or in the soda-lime “B” case, a metal) was deposited before the Mo back contact and no sodium was deliberately added, (b) the barrier was omitted and no sodium added, (c) the barrier was used and a small amount of sodium was added to the copper deposition source, and (d) the barrier was omitted and sodium added. The rest of the cell fabrication was done with as nearly identical processing as possible.

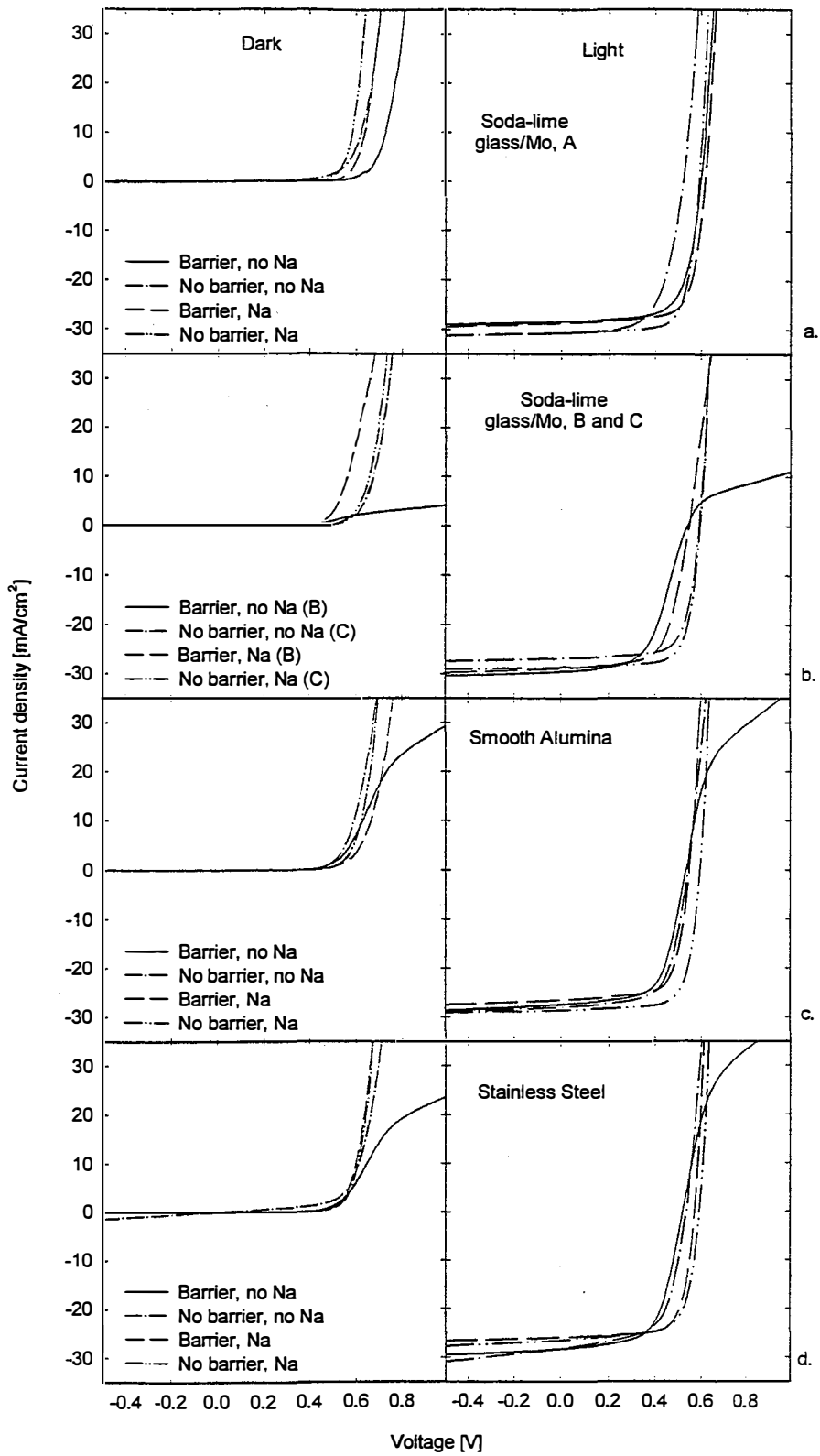
Current-voltage curves for the different substrates and different sodium conditions are shown in Fig. 1. In the future, the amounts and profiles of Na will be measured, but at present only qualitative labels are used. In several cases where a diffusion barrier was used, and no sodium deliberately added, there was significant current limitation in forward bias for both light and dark measurements. Individual parameters deduced from the Fig. 1 data showed significant cell-to-cell variation, but also clearly identifiable trends that qualitatively tracked the assumed sodium concentration.

Fig. 2a and 2b show the two primary indicators of junction quality, open-circuit voltage and fill factor, for the different substrates and sodium concentrations. The trend for both voltage and fill factors to increase when more sodium is present. Fig. 2c shows that the combination of these two effects is a fairly clear increase in cell efficiency with greater amounts of sodium. No significant variation in CIGS bandgap, as deduced from quantum efficiency, was seen among the cells depicted in Figs. 1 and 2, and the small variation in current density did not appear to correlate with sodium content.

---

<sup>1</sup> J.R. Tuttle, et.al. *IEEE PVSC* **25**, 797 (1996).

<sup>2</sup> J.E. Granata, J.R. Sites, and J.R. Tuttle, *AIP Conf. Proc.* **394**, 621 (1996).



**Figure 1. Current-voltage curves for CIGS cells with five substrates and four sodium conditions. “No Na” means none deliberately added.**



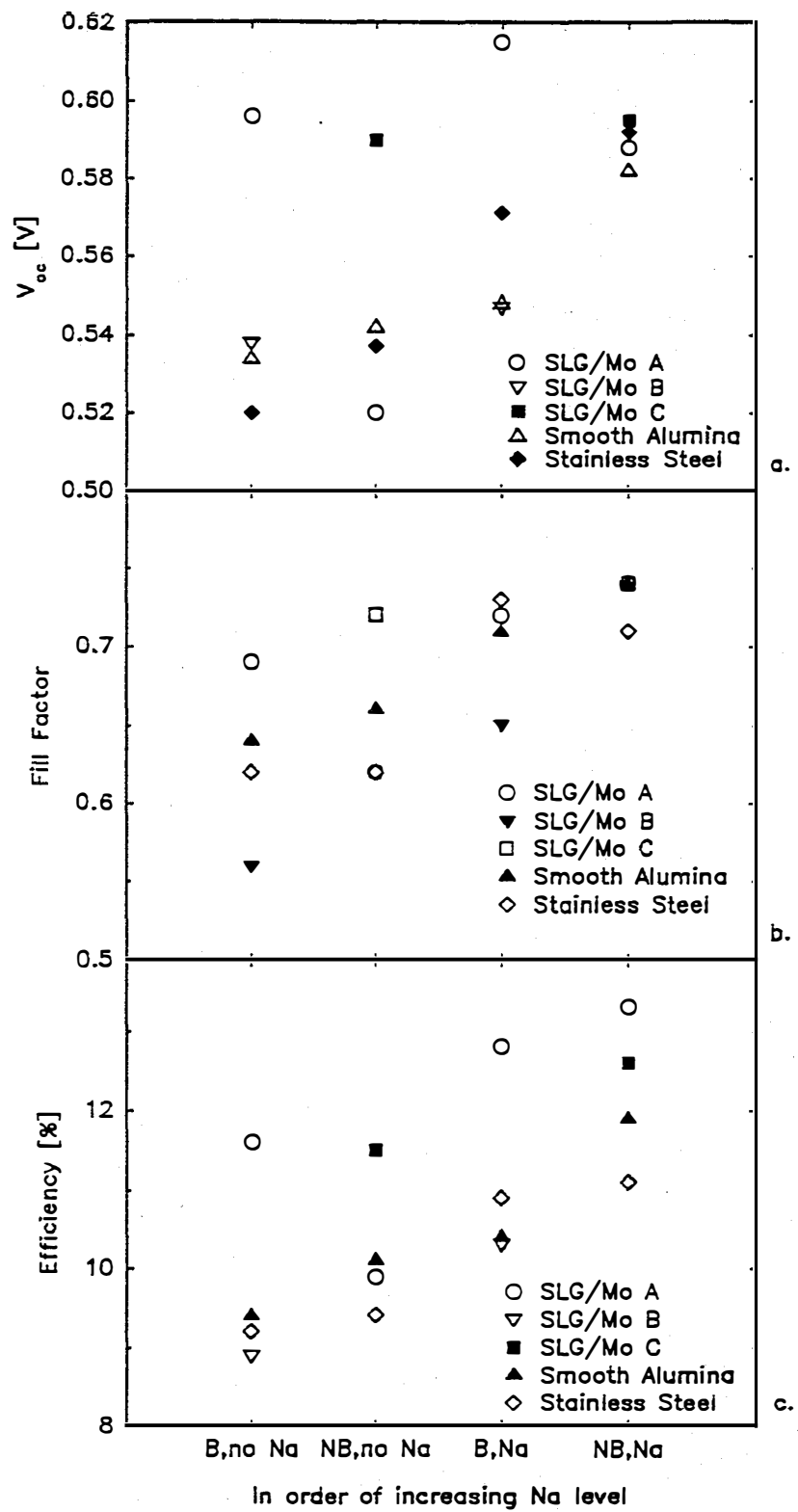
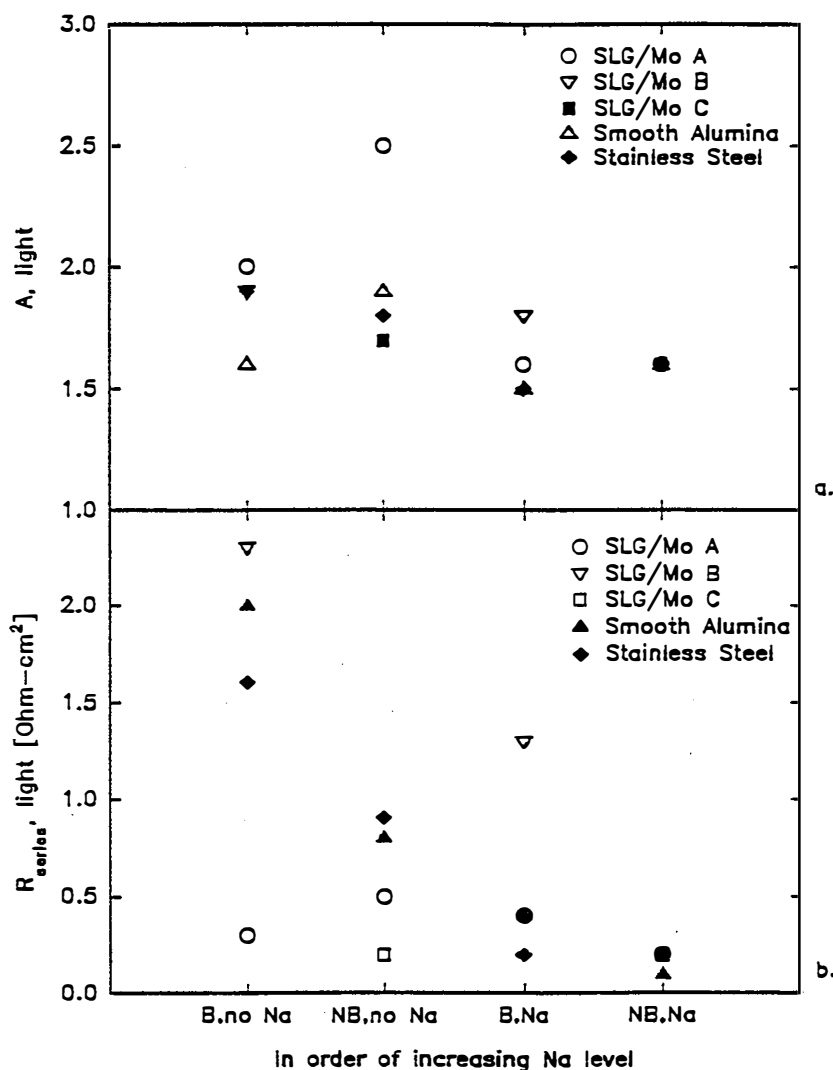


Figure 2. Trends observed in (a) open-circuit voltage, (b) fill factor, and (c) efficiency of CIGS cells with increasing sodium concentration.

Two major factors in determining fill factor are shown in Fig. 3. The diode quality factor  $A$  under illumination generally decreases when more sodium is present. The series resistance  $R$ , also has a downward trend, though the large values at the left of the plot correspond to the current-limited curves in Fig. 1 and therefore have considerably more uncertainty.



**Figure 3. Trends observed in (a) diode quality factor and (b) series resistance under illumination for same CIGS cells.**

A final comparison, shown in Fig. 4, is hole density in the CIGS absorbers deduced from capacitance measurements. The larger hole densities in the higher-sodium, better-junction cells is the correlation

most often seen. The most likely physical interpretation is less compensation due to fewer extraneous donor states, and hence a lower forward recombination current.

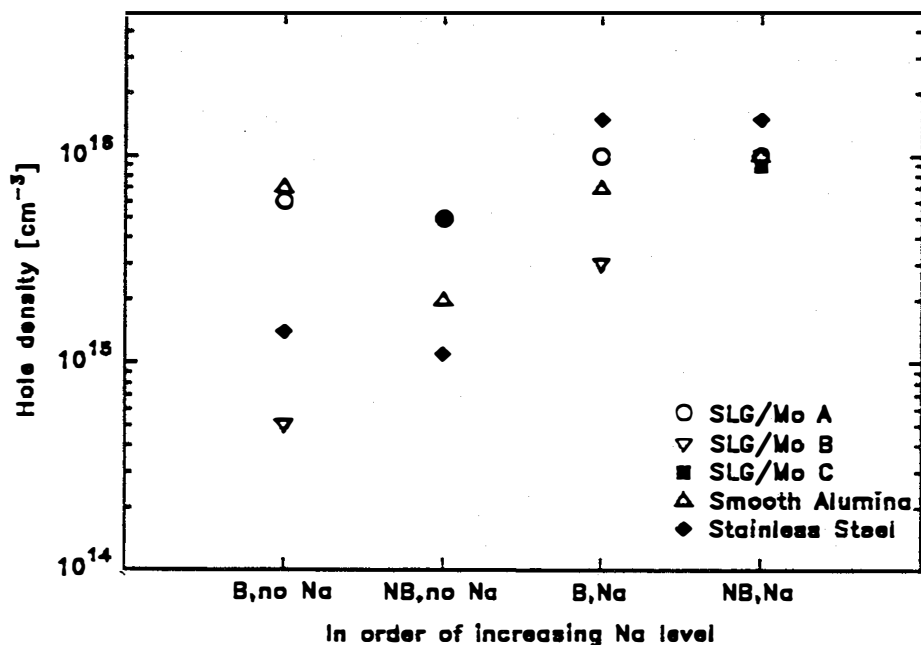


Figure 4. Trend observed in CIGS hole density with increasing sodium concentration.

Continuing work in this area will introduce much more quantitative amounts of sodium. It will also utilize SIMS analysis to determine the spatial profiles of sodium in actual cells and to give another indicator of relative sodium concentration. Similar studies will be made with  $\text{CuInSe}_2$  absorbers without gallium. One reason to use pure CIS is the practical consideration that it is much easier to control the process, and hence reduce cell-to-cell variations, with one fewer element involved. A second reason is that since both CIS and CIGS are candidates for commercial cells, it is important to know whether or not the sodium effect is modified by the presence of gallium. Also for future studies, one must logically ask whether the positive effect of sodium is unique, or whether there are other elemental impurities that might have a similar, or perhaps even more positive, effect on cell performance.

# CELL ANALYSIS

## CIS/CIGS

Colorado State participated in the characterization of CIGS cells fabricated by Raghu Bhattacharya of NREL by electrodeposition (10/22/96 report to Bhattacharya). Three different gallium concentrations were used. Fig. 5a shows the light current-voltage curves for one cell from each concentration, and Fig. 5b shows the corresponding quantum efficiency curves. In all cases, efficiencies were in the 12-14% range. Bandgaps deduced from the long-wavelength quantum-efficiency cutoffs were 1.07, 1.13, and 1.22 eV for these three cells. The current-voltage curves, which show a progression to higher voltage and smaller current, reflect this variation.

Fig. 6 compares open-circuit voltage with bandgap for the three gallium concentrations used for the electrodeposited CIGS cells. The differences between  $qV_{oc}$  and  $E_g$  are 0.52-0.54 eV. Also shown on the same plot is the progression of record-setting, or near-record-setting, CIGS cells made at NREL by evaporative techniques. The smallest  $qV_{oc}$ - $E_g$  difference is 0.47 eV. The dashed line is simply an aid to the eye, which corresponds to a difference of 0.5 eV. The results from the electrodeposited CIGS should be viewed as quite good. The 50 mV difference in  $V_{oc}$  with the best cells made is remarkable for a technique that has not to date received a large amount of development investment. Particularly noteworthy is the 700 mV cell (open circle) which has a modest  $qV_{oc}$  - $E_g$  differential at a relatively large gallium concentration.

A second characterization study involved CIS cells fabricated at Solarex (8/5/96 report to John Kessler). In this case, the focus was comparative study of the value of a high-resistivity ZnO layer between the CdS layer and the conducting ZnO front contact. Three cases were compared: A had no high-resistivity ZnO, B had a high-resistivity layer with additional oxygen added during deposition, and C had a high resistivity layer deposited without additional oxygen. In each case, different thicknesses of CdS were used corresponding to 0 (no CdS at all), 2, 3, 4, and 8 minutes of chemical-bath deposition (CBD) times.

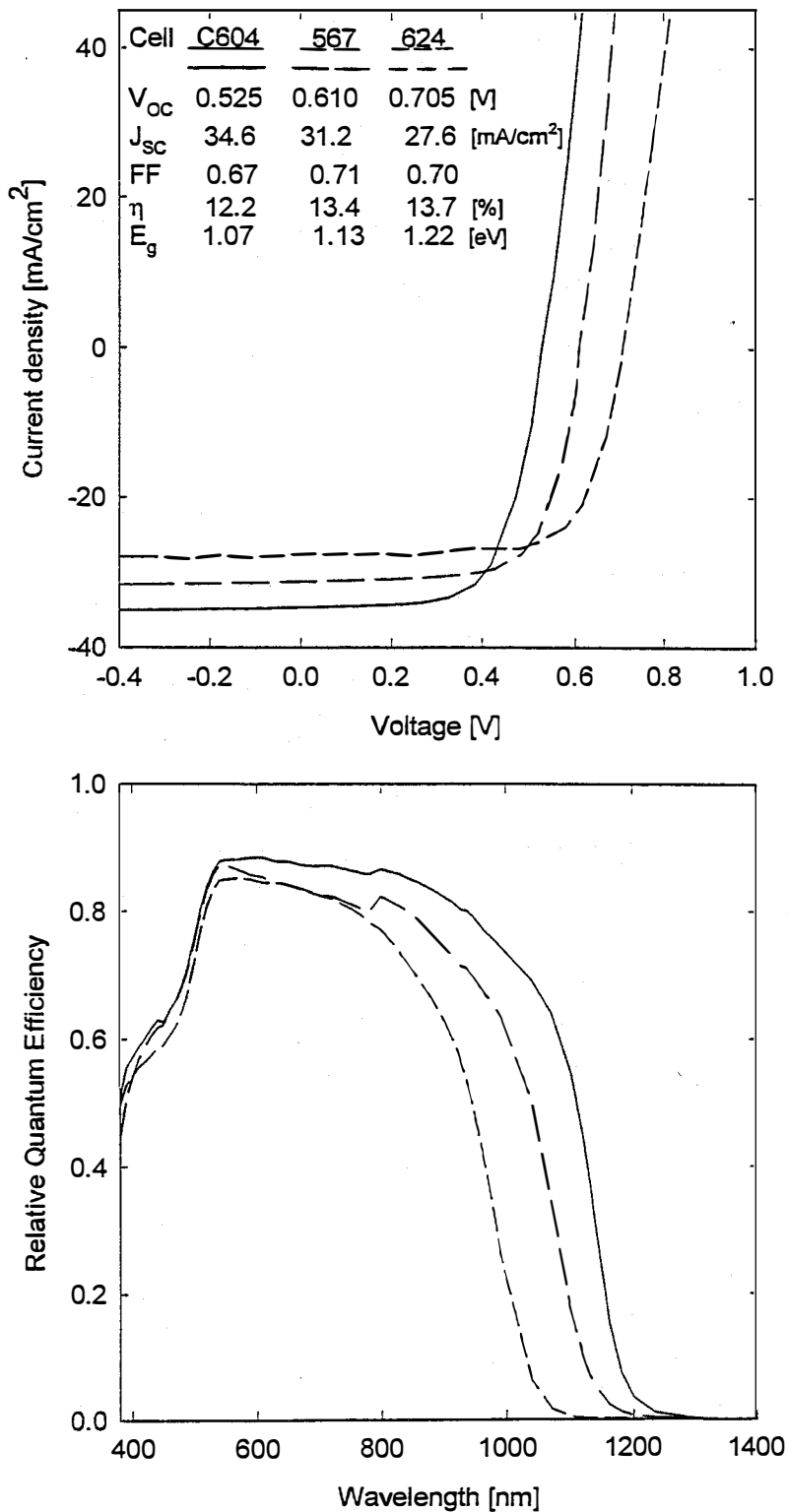
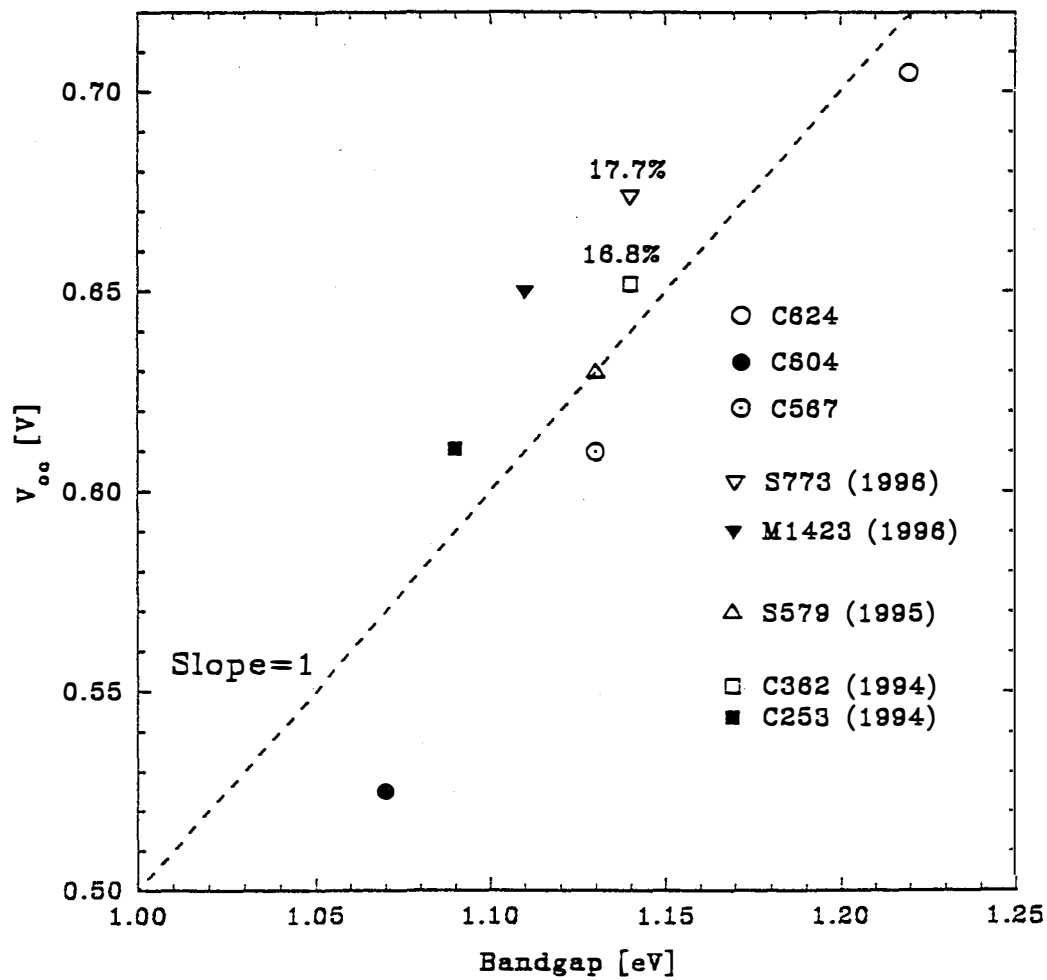


Figure 5. (a) Current-voltage curves for CIGS cells fabricated at NREL by electrodeposition. (b) Corresponding quantum efficiency curves for the three gallium concentrations used.



**Figure 6. Open-circuit voltage vs. bandgap for electrodeposited (circles) and other high-efficiency CIGS cells made at NREL.**

Fig. 7 shows the key solar-cell parameters from one cell per substrate, for the different ZnO conditions and CdS deposition times. The cells with CBD deposition times greater than 2 min have

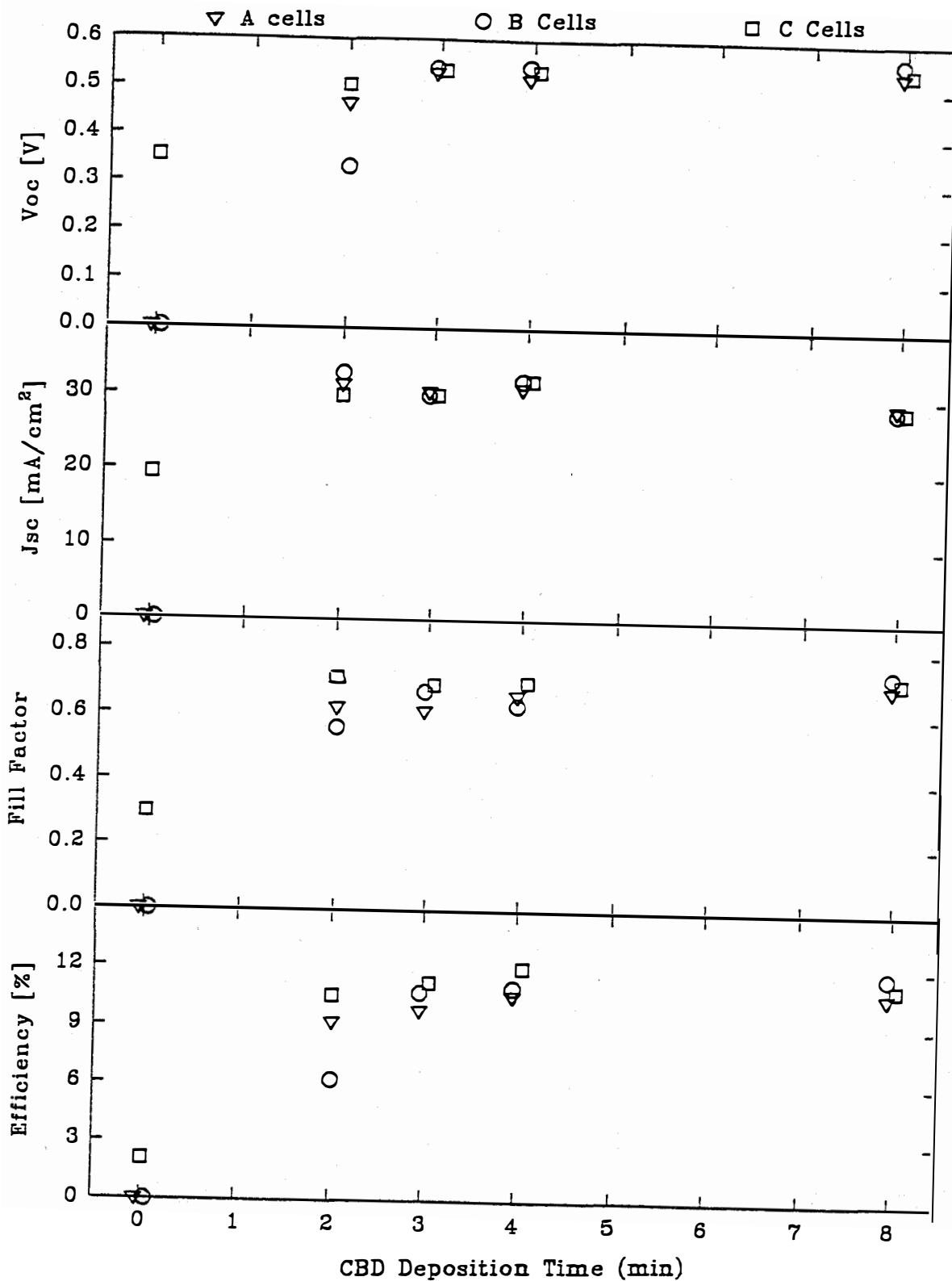


Figure 7. Variations in key parameters of Solarex CIS cells with the use or non-use of a high-resistivity ZnO layer and with the CdS deposition time.

similar parameters and the presence of high-resistivity ZnO does not appear to be significant, though it may reduce shunting somewhat. Quantum efficiency as expected showed less blue response with thicker CdS. All these efficiencies were between 10 and 12%. With thinner CdS, or none at all, the cells do not perform as well. The 2-min cells had lower voltage and fill factor. In the extreme case, the cells in this study that had neither CdS nor a high-resistivity ZnO layer showed no photovoltaic response.

A third CIGS study involved cells both fabricated and measured at NREL (12/13/96 report to Noufi and several others). The purpose of this study was to see whether there was any significant difference between the highest-efficiency cells made with the three commonly used NREL deposition systems, referred to internally as S, C, and M. Fig. 8a overlays the current-voltage curves for the best cells from each system, and Fig. 8b shows the corresponding quantum efficiencies. Superimposed on the quantum-efficiency curves is the estimated grid loss and the measured reflection from one of the cells.

The two cells NREL made in 1996 are about 20 mV higher in open-circuit voltage without an obvious difference in the bandgap of 1.14 eV deduced from the quantum efficiency cutoff. The two newer cells also have the same current and essentially identical QE curves. These curves imply an internal quantum efficiency very nearly unity between 550 and 750 nm. The older cell has a QE a few percent lower over this range.

Fig. 9 shows the forward current for the three cells on a logarithmic scale using the same data shown in Fig. 8a. The fits after removal of the resistive terms are essentially identical for the two newer cells, and the older one is parallel but 20 mV lower in voltage, or equivalently 40% larger in forward current. All three slopes correspond to a diode quality factor of 1.5. Resistive corrections are fairly small: the largest series resistance (S573) reduces efficiency by just over 0.1%, and the smallest shunt resistance (M1574) reduces efficiency by just over 0.2%. In the absence of these resistive corrections, all three fill factors would be slightly above 0.78.



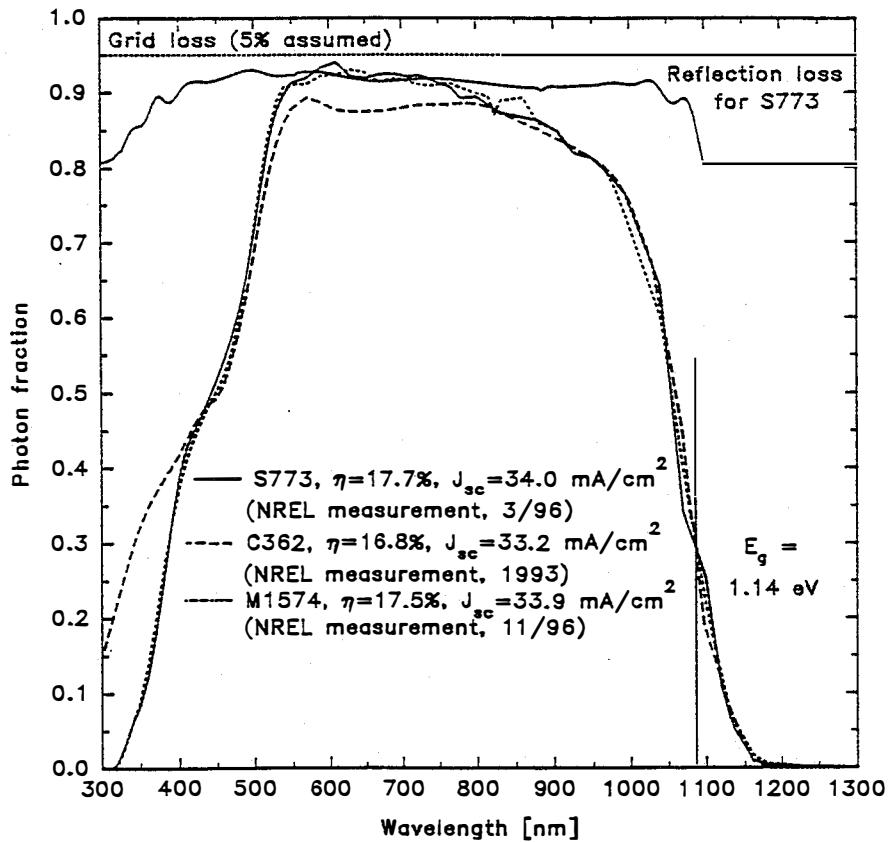
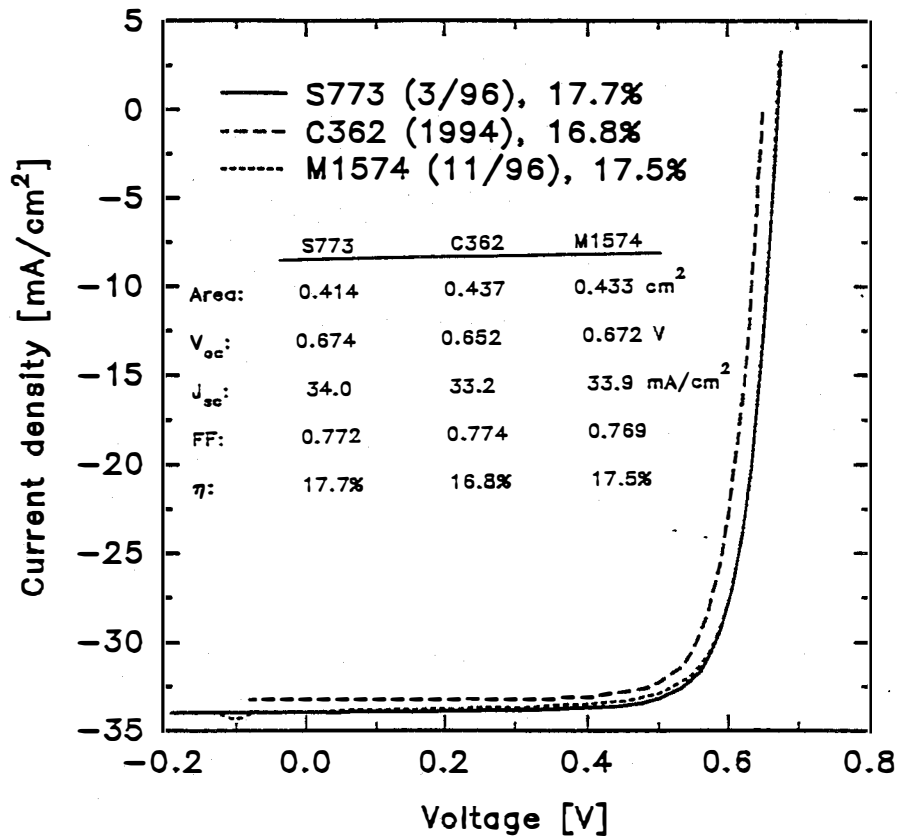


Figure 8. Comparison of (a) current-voltage curves, and (b) quantum efficiencies for the highest efficiency CIGS cells deposited with the three primary NREL systems.

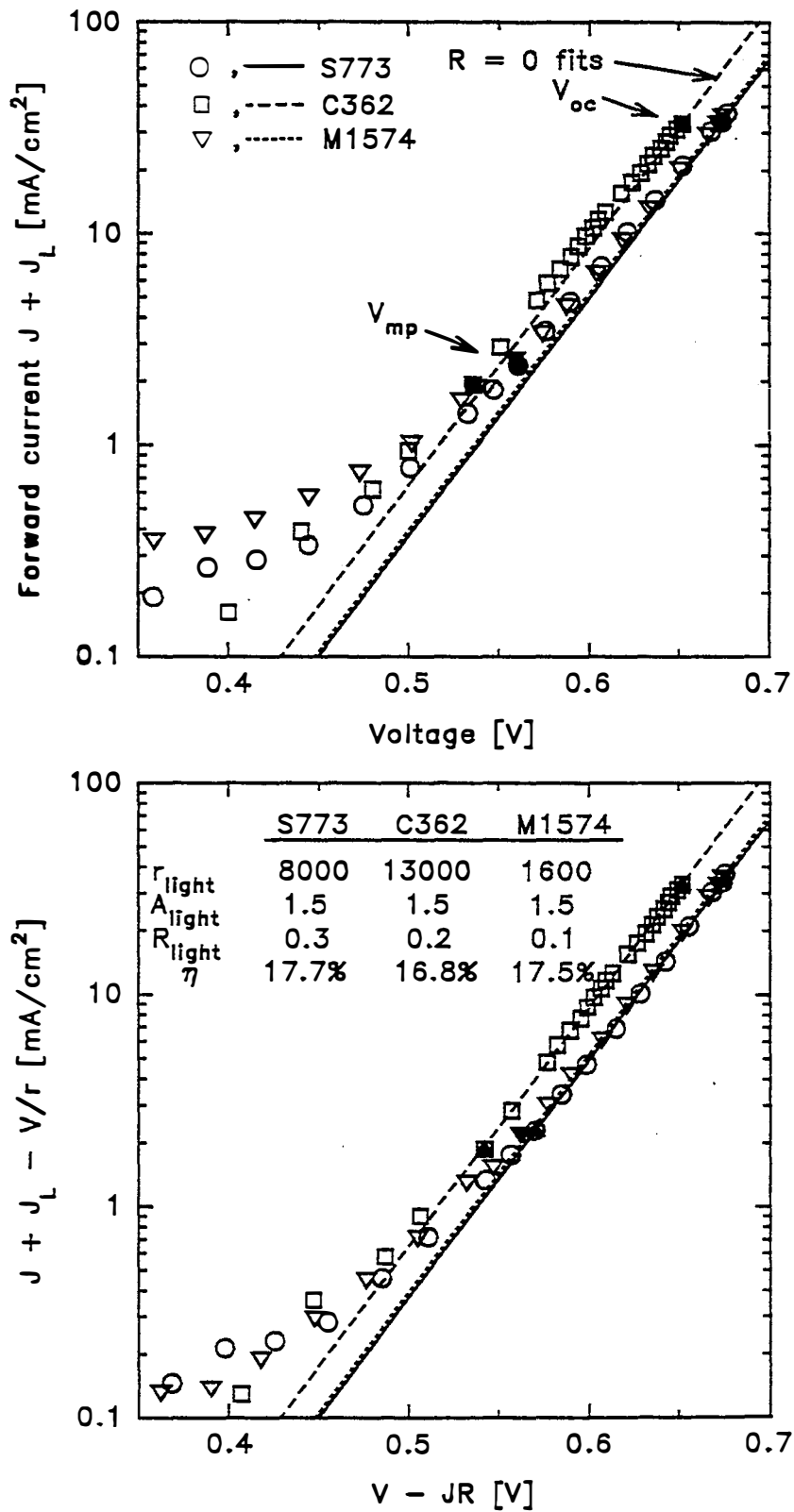


Figure 9. Logarithmic presentation of the data from Fig. 8a. Top part shows uncorrected data and bottom shows same data with resistive corrections.

## CdTe

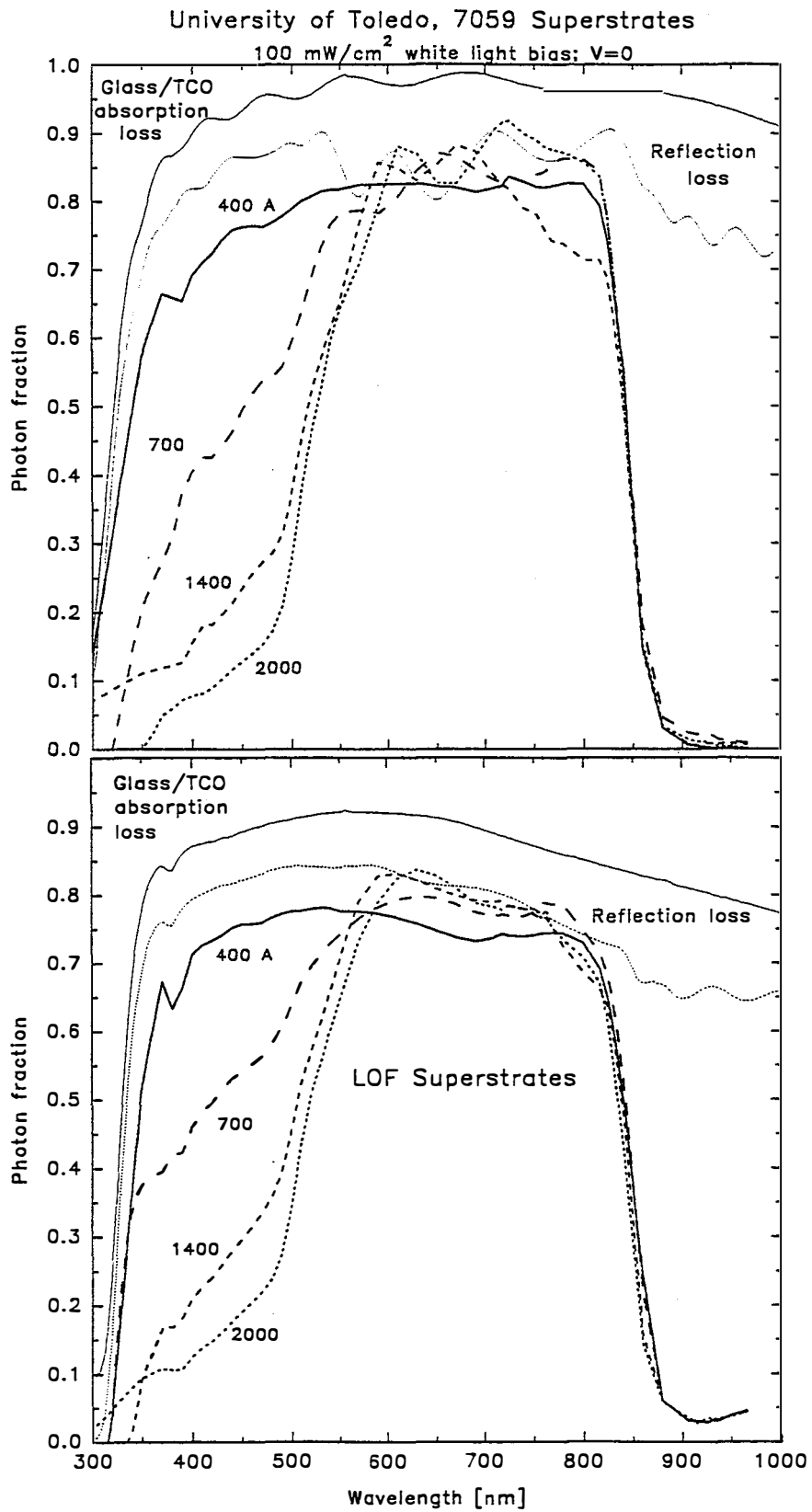
The major CdTe project for 1996, which was a central part of the team activity, was the comparison of cells that were nominally identical except for thickness of the CdS window. In the first round, cells with CdS thicknesses between 500 and 2500 Å were fabricated by NREL, University of Toledo, Solar Cells, Inc., University of South Florida, Colorado School of Mines, and the Institute of Energy Conversion (1/22/96 and 5/15/96 CdTe Team Meeting Reports). In the second round, these laboratories, plus Golden Photon, Inc., provided cells with the CdS thickness specifically targeted to be 200 and 800 Å (11/18/96 CdTe Team Meeting Report).

Fig. 10 shows the comparison of the quantum efficiencies from the first-round cells made at the University of Toledo.<sup>3</sup> Two superstrates and four CdS thicknesses are shown. Measured superstrate absorption and completed cell reflection are plotted downwards to indicate the photon losses from these sources. The LOF superstrates have a significantly higher current loss (about 3.5 mA/cm<sup>2</sup>) due to absorption. The CdS absorption loss ranged from about 5 mA/cm<sup>2</sup> for the thickest CdS shown in Fig. 10 to about 2 mA/cm<sup>2</sup> for the thinnest. Current-voltage measurements made on the round one cells showed a tendency for the voltage and fill factor to deteriorate for the thinnest cells. The onset of this deterioration generally occurred between 500 and 1000 Å and appeared to be less serious for cells fabricated by close-spaced sublimation.

In the second round of measurements with thinner CdS cells, it was realized that the thickness of the CdS after completion of the cell was generally less than that which was deposited. Thus, the parameter adopted to describe CdS thickness was the percentage of blue-photon absorption, which is defined at the top of Fig. 11. The hand-drawn lines are quantum efficiencies near 450 and 600 nm. The fill factor and open-circuit voltage for the round two cells are plotted against this parameter in the bottom section of Fig. 11. A 40% blue-photon absorption corresponds roughly to a CdS thickness of 1000 Å. This plot shows that fill factor and voltage generally decrease when thinner CdS is used. Not shown in Fig. 11, however, is the recent high-efficiency cell made at Golden Photon, where the blue-photon absorption is essentially zero, but the fill factor and voltage are similar to the values shown for other cells with blue-photon absorption of 40-50%.

---

<sup>3</sup> J.E. Granata, J.R. Sites, G. Contreau-Puente, and A. D. Compaan, *IEEE PVSC* **25**, 853 (1996).



**Figure 10.** Comparison of quantum-efficiency curves for different thickness CdS in CdTe cells fabricated at the University of Toledo on two types of glass superstrate.

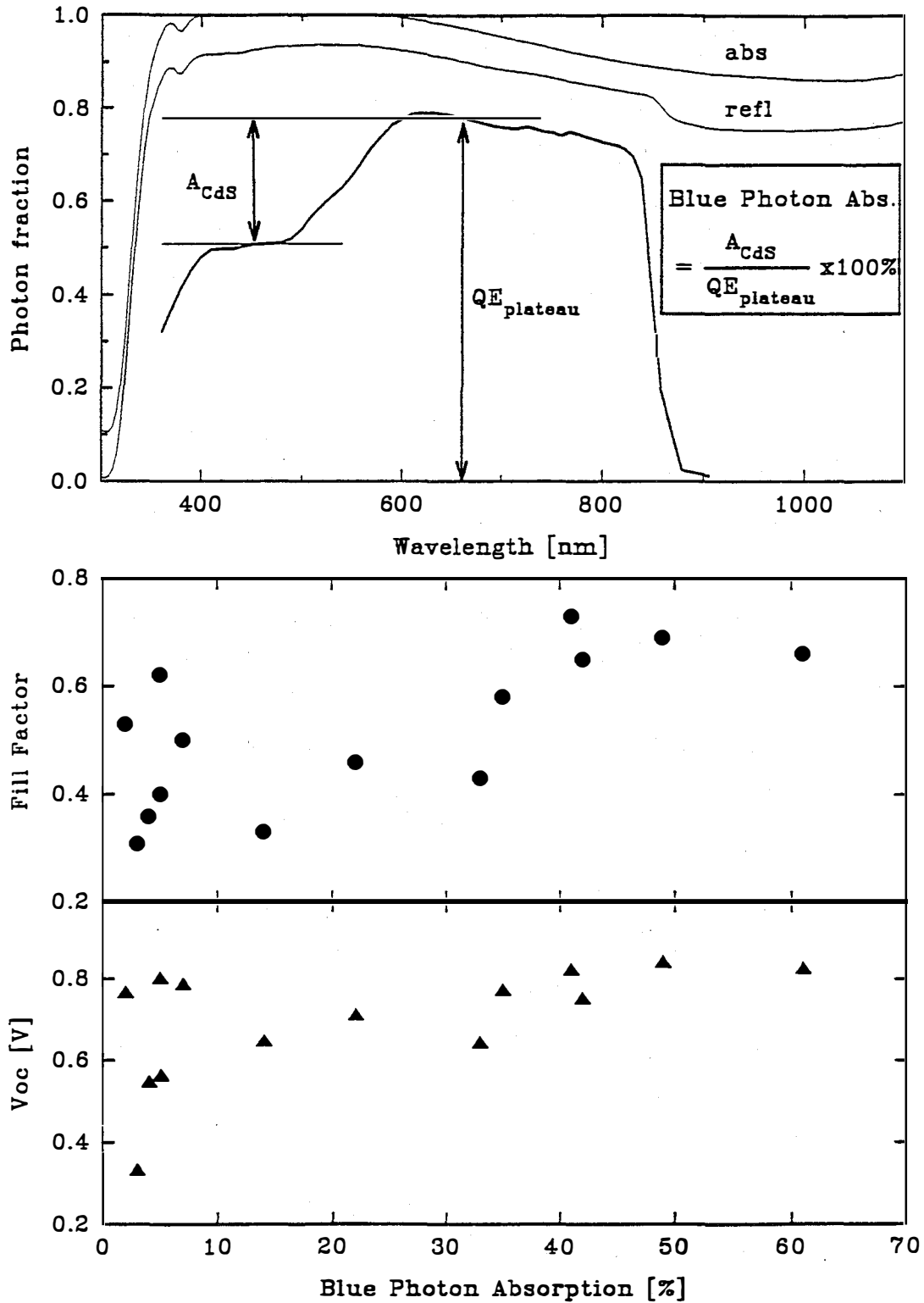


Figure 11. CdTe cell voltage and fill factor as a function of CdS blue-photon absorption as defined by the top diagram. Cells are from seven laboratories.

The current-voltage curve of the high-efficiency Golden Photon (GPI) cell is shown in Fig. 12 in comparison to the highest-efficiency CdTe cell from the University of South Florida (USF), the record-efficiency crystalline GaAs cell, and the calculated maximum cell response for the CdTe bandgap. The GPI and USF curves are fairly similar and show a trade-off between current and voltage.

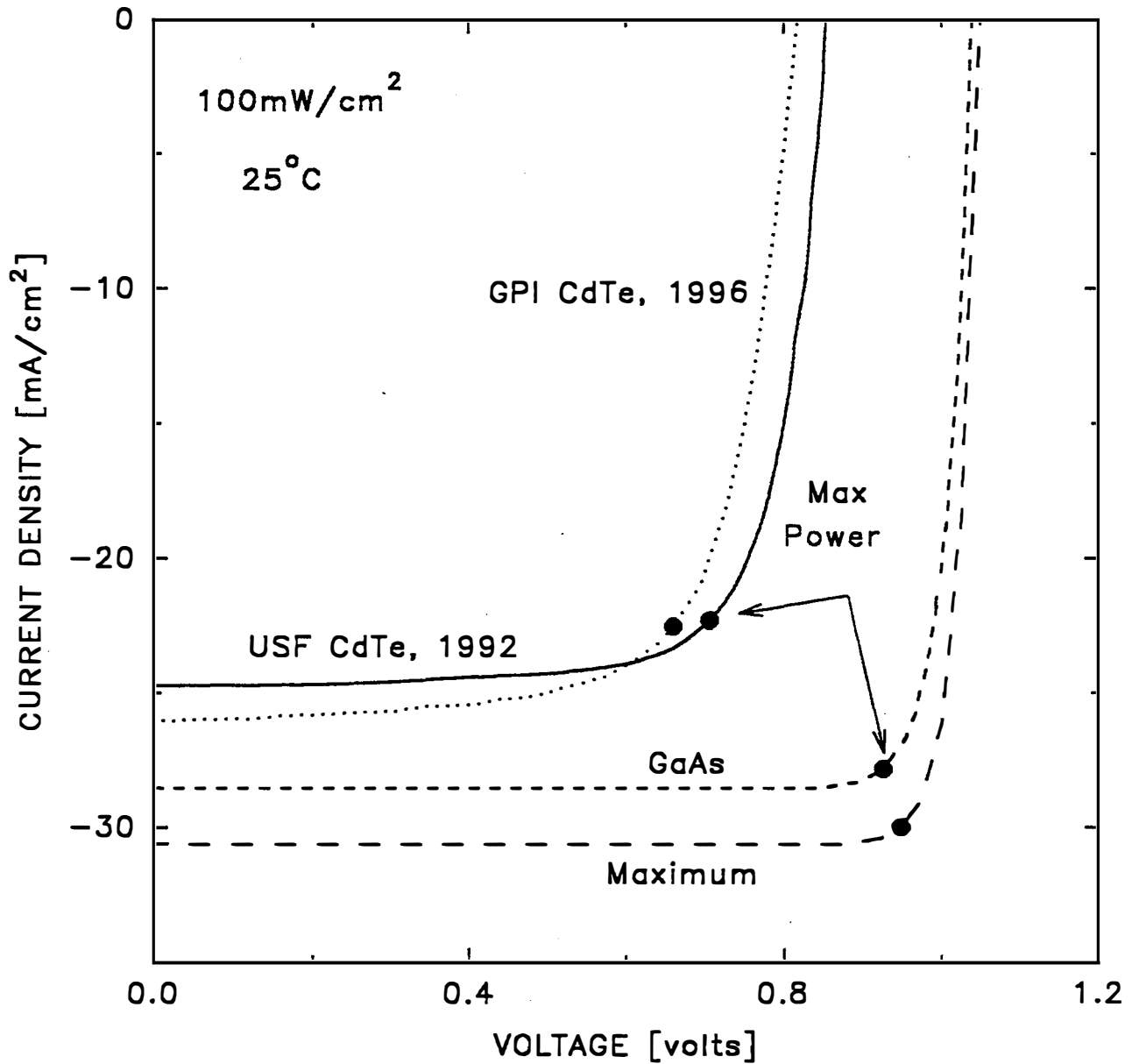


Figure 12. Comparison of high-efficiency CdTe cells from USF and GPI. GaAs and calculated maximum shown for reference.

The lower voltage, higher current for the GPI cell is due to a reduced bandgap, which is a result of sulphur diffusion into the CdTe to produce a CdTe<sub>1-x</sub>S<sub>x</sub> layer. The reduction in bandgap is confirmed in Fig. 13, which overlays the bandgap cutoff in quantum efficiency of the two cells. The wavelength difference between the two is 19 nm, which corresponds to a bandgap difference of 32 meV. This difference is very nearly the bandgap difference between the two cells. The increased photocurrent available to the GPI cell with the 32 meV smaller bandgap is about 1.2 mA/cm<sup>2</sup>, again similar to that seen in Fig. 12. However, superstrate transmission and quantum-efficiency measurements show that the photocurrent losses are somewhat different between the two cells. The GPI cell has a greater superstrate/TCO absorption loss, whereas the USF cell has a greater short-wavelength loss due to CdS absorption.

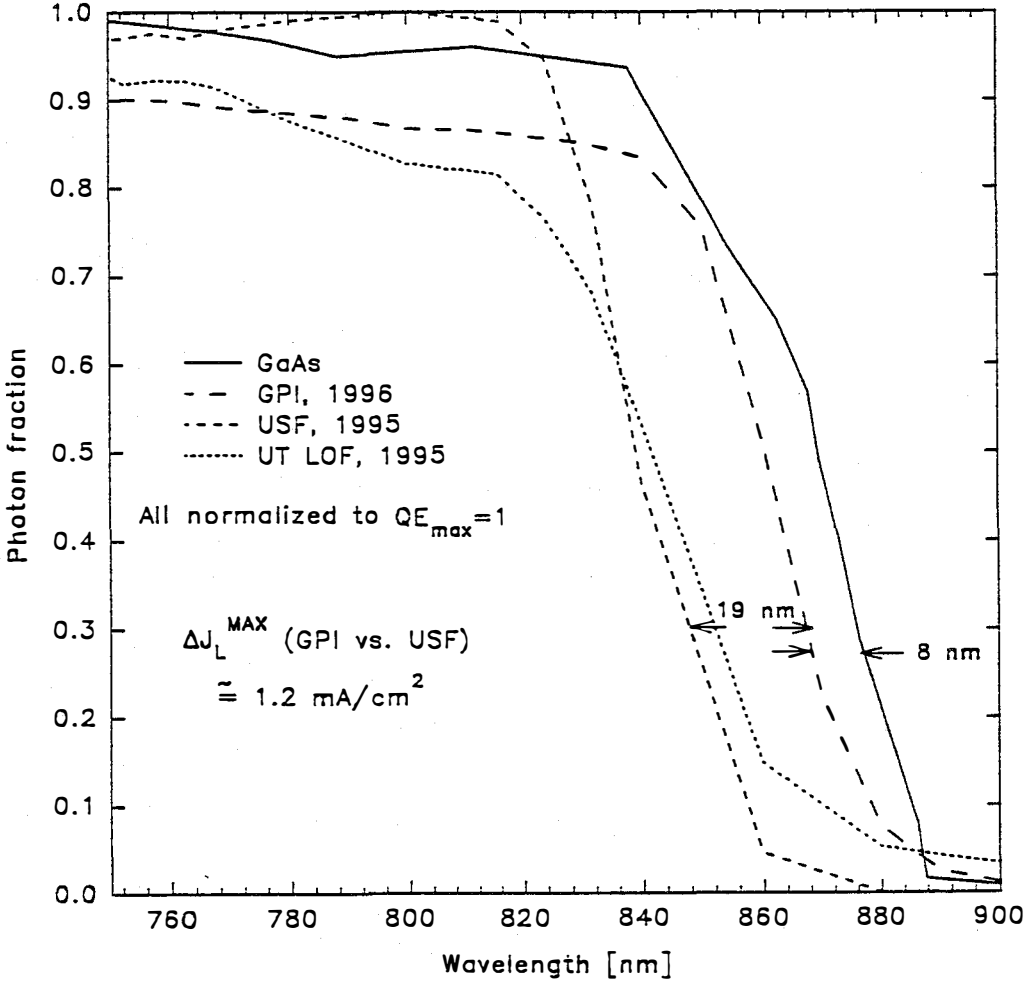


Figure 13. Comparison of quantum-efficiency cutoffs for high-efficiency CdTe cells.

There is also a difference in fill factor between the GPI and USF cells. This difference is best illustrated by a logarithmic plot of forward current density ( $J+J_L$ ) vs. voltage as shown in Fig. 14. The data, as well as the crystalline GaAs and calculated maximum, are the same as in Fig. 12. The dashed lines are fits for zero series resistance and infinite shunt resistance. The slopes are very nearly equal for the two CdTe cells, corresponding to diode quality factors of 2.1 for GPI and 2.0 for USF, and the difference between the dashed lines is the 32 meV bandgap difference. The GPI data, however, deviates more from the fit, near  $10\text{mA/cm}^2$ , implying a somewhat higher series resistance ( $1.2\ \Omega\text{-cm}^2$ ) than that of the USF cell ( $0.5\ \Omega\text{-cm}^2$ ). The large deviations from the fits below  $V_{MP}$  are primarily leakage effects.

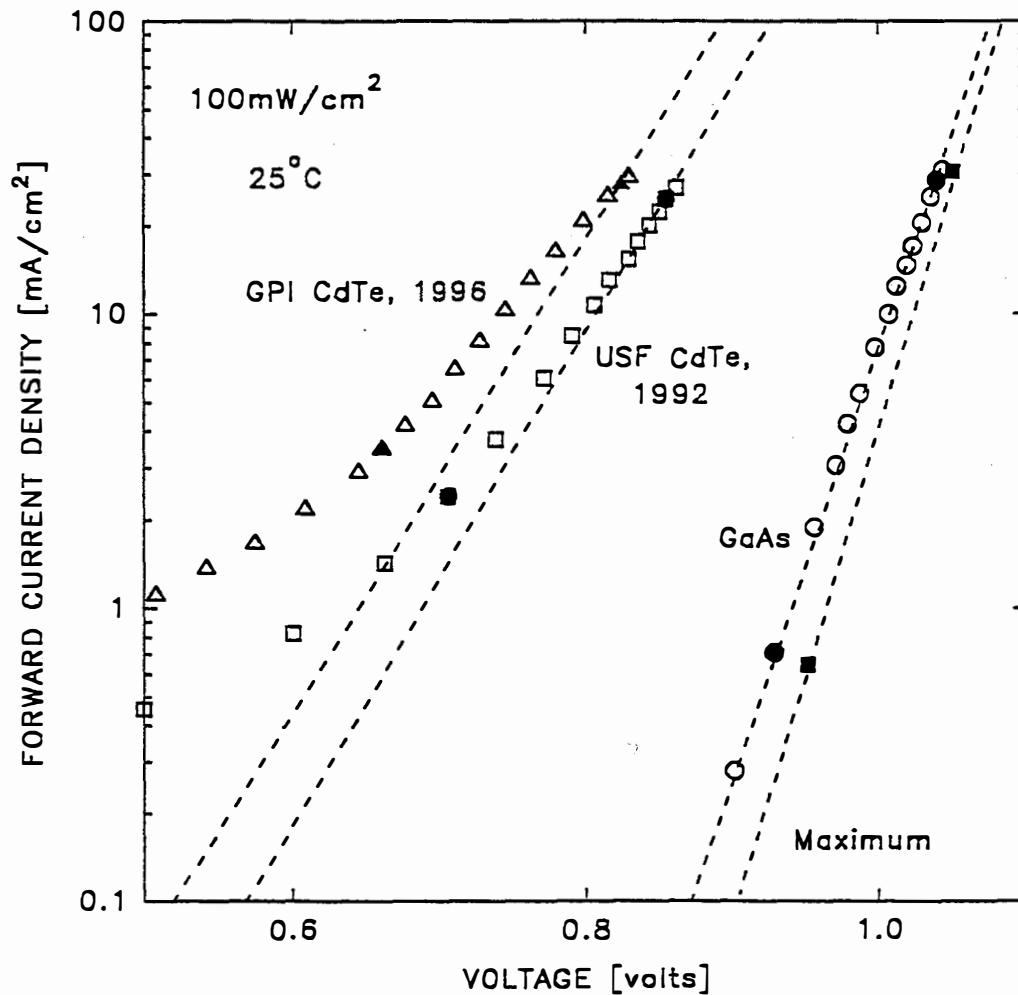
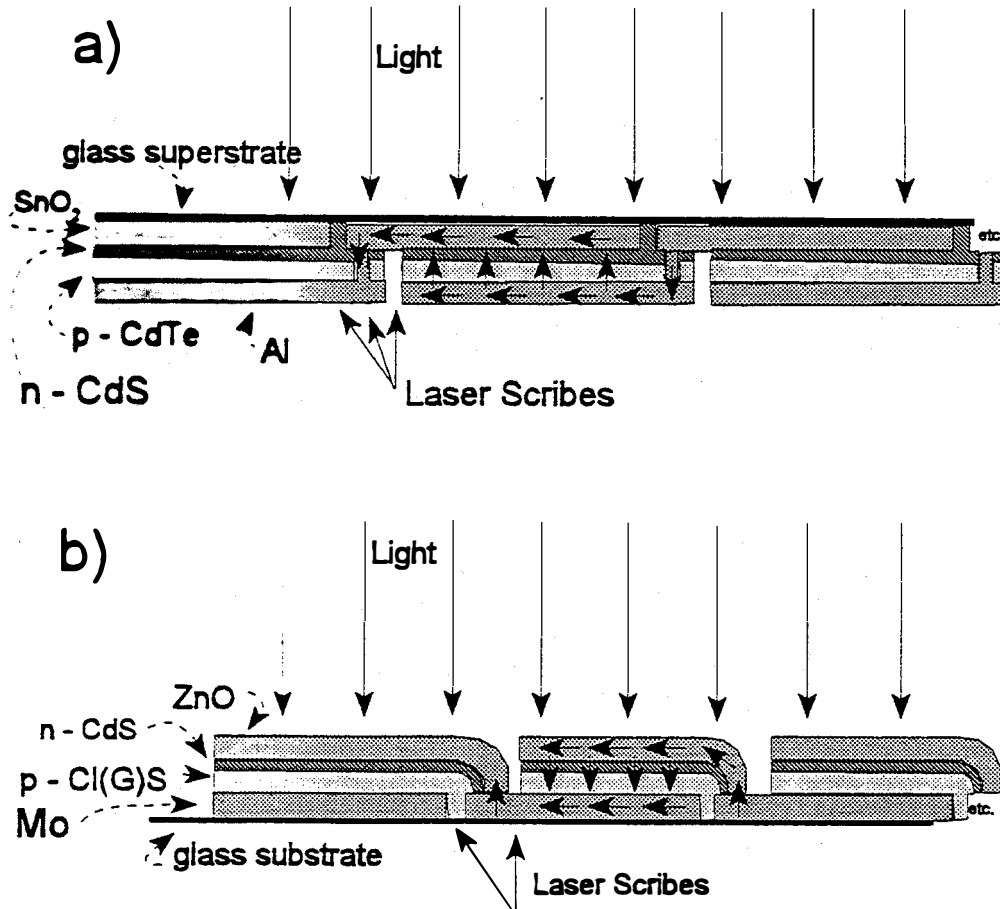


Figure 14. Data from Fig. 12 plotted as  $\log(J + J_L)$  vs.  $V$ .



## MODULE ANALYSIS

A series of investigations of thin-film polycrystalline modules were completed by Ingrid Eisgruber.<sup>4</sup> Fig. 15 shows the CdTe and Cu(In,Ga)Se<sub>2</sub> module-interconnect configurations commonly used. In both cases, three scribing steps are required to separate the individual cells and electrically reconnect



**Figure 15. Standard interconnect patterns for CdTe and CIGS thin-film modules.**

them in series. The light is either a broad, solar-like source or a laser beam that is scanned across each cell in the module. The latter procedure was done on a large number of modules in collaboration with Richard Matson at NREL. The optics system, which can scan over a meter in two directions, is shown schematically in Fig. 16.

<sup>4</sup> I.L. Eisgruber, IEEE PVSC 25, 829 (1996).

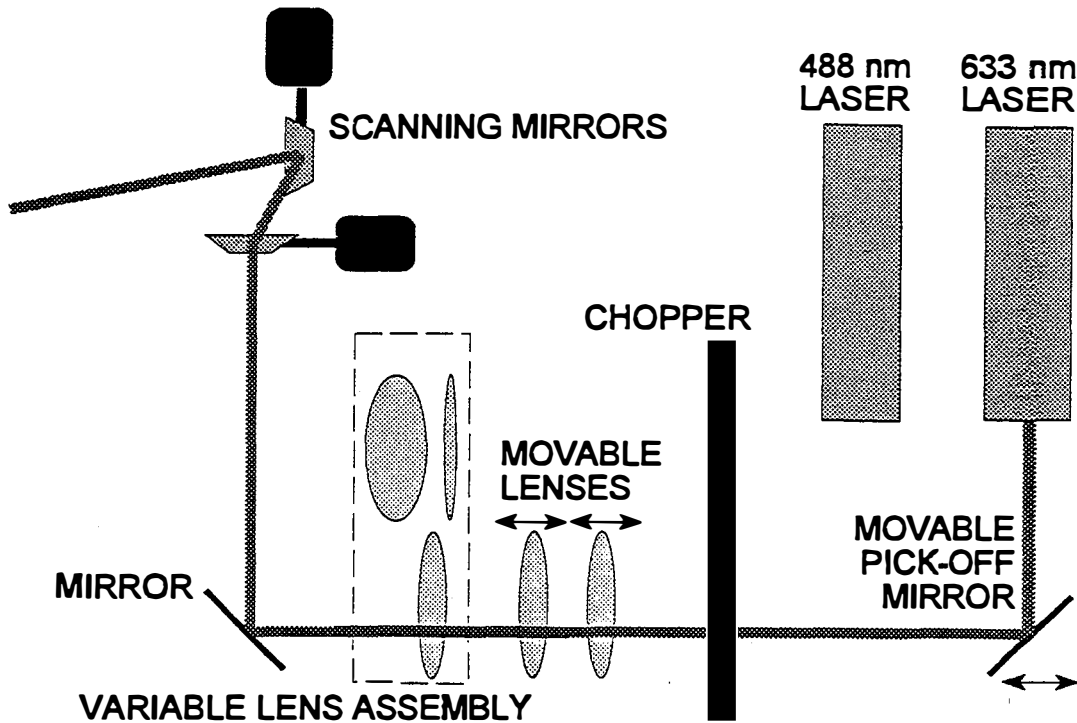
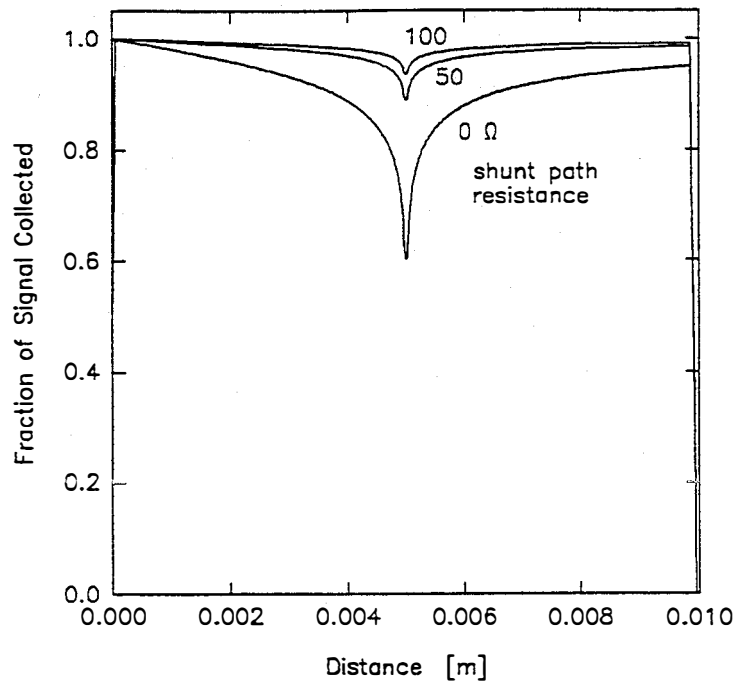


Figure 16. Schematic of large-scale laser scanner at NREL.

Laser scanning is basically a measure of the photo-current induced by a focused beam as it is directed across a cell or module. A primary use of laser scanning in module analysis is the identification of the location and the nature of defects. There tend to be a high density of defects in the vicinity of a module's scribe lines used to define the interconnects. In practice these lines are not as clean as suggested by Fig. 15.

Cell defects can be loosely divided into local shunts and local areas of reduced photocurrent. Fig. 17 shows the calculated impact on the photocurrent when the beam passes over 2  $\mu\text{m}$  diameter shunts of varying resistance. The characteristic signature is a gradual decrease in signal over a 1 mm distance scale. Clearly, however, the shunt needs to have a very low resistance to have much impact on the scan. In contrast, a photocurrent defect often yields near-zero signal over the area of the defect and little or no impact elsewhere.



**Figure 17.** Calculated laser-scan signal for a 1 cm wide CdTe cell with a 2 μm diameter shunt.

A combined shunt-photocurrent defect was deliberately introduced to a CIS cell by pricking it with a pin. The resulting shunt resistance was determined to be 14000 Ω (much less of a shunt than any shown in Fig. 17), its diameter was 300 μm, and the transition from full to zero photocurrent was very abrupt. This observation is consistent with the calculation shown in Fig. 18, which shows the

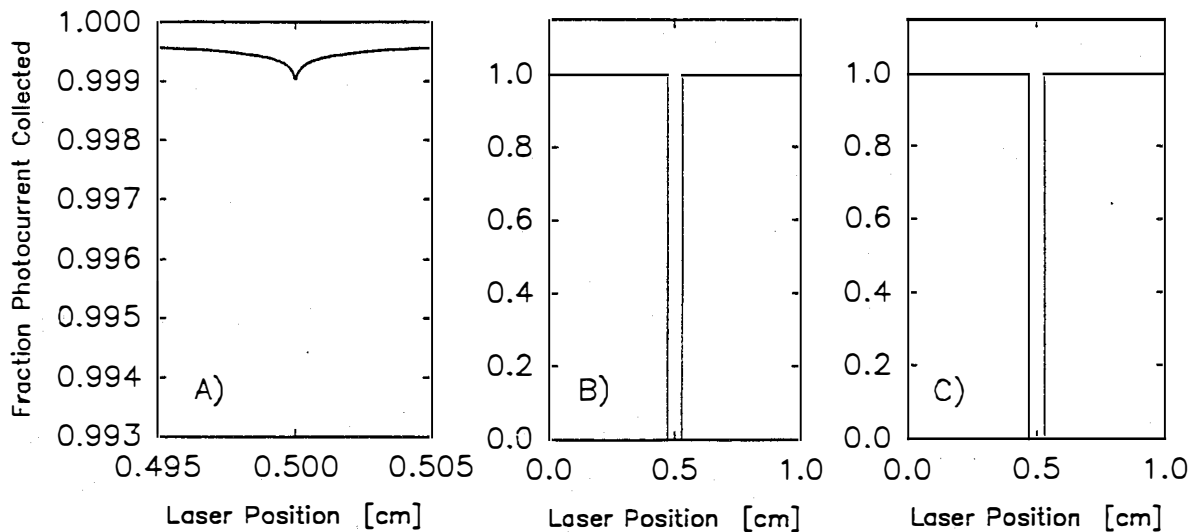


**Figure 18.** Calculated signature of (a) a 14 KΩ shunt, (b) a 300 μm photocurrent defect, and (c) a combination of the two.

effect of the shunt to be negligible compared to the loss of photocurrent. Furthermore, although both are present, the only practical consequence is the local loss of photocurrent.

Measurement of current-voltage curves for individual cells in a thin-film module must be done with care. Since the cells are typically quite long compared to their width, a two-wire measurement, between B and C in Fig. 19 for example, will include excess series resistance due to the long path length to reach the top and bottom of cell #2. The extra resistance,  $\rho_s L^2/12$  is the order of  $100 \Omega\text{-cm}^2$  for even a small module with  $L \approx 10 \text{ cm}$  and  $\rho_s \approx 10 \Omega/\text{sqr}$ . Clearly one needs to use the low-resistance metal contacts (A and D) to the end cells for the current leads and then measure the voltage at B and C, or across any other cell, with separate leads.

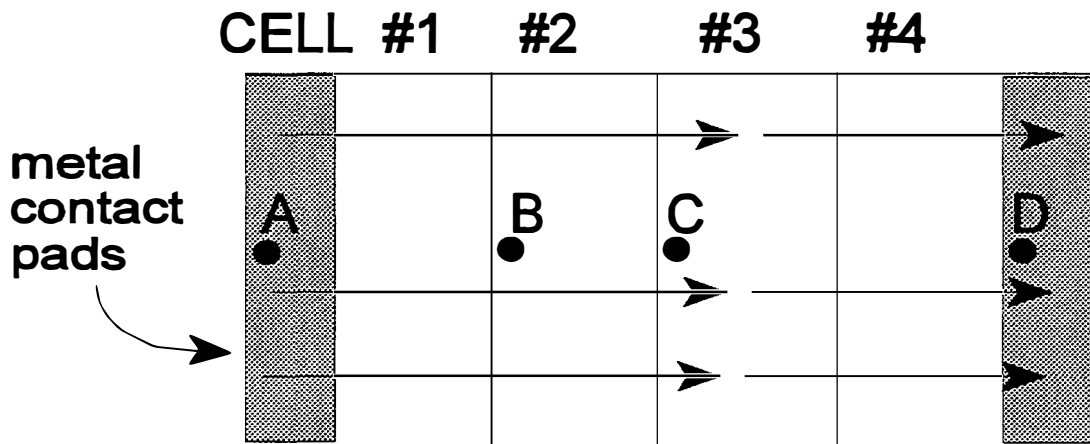


**Figure 19. Schematic of four-cell module.**

In addition, the voltage drop across the width of a module cell is likely to be significant, and even with a four-wire measurement, the voltage probes must be placed properly. This point is illustrated in Fig. 20, where a two-cell module is shown for simplicity. The current leads are at the ends as described above, and one voltage lead is assumed to be at the right end also. The placement of the other lead at F or G, however, can produce radically different current-voltage curves. Placement of

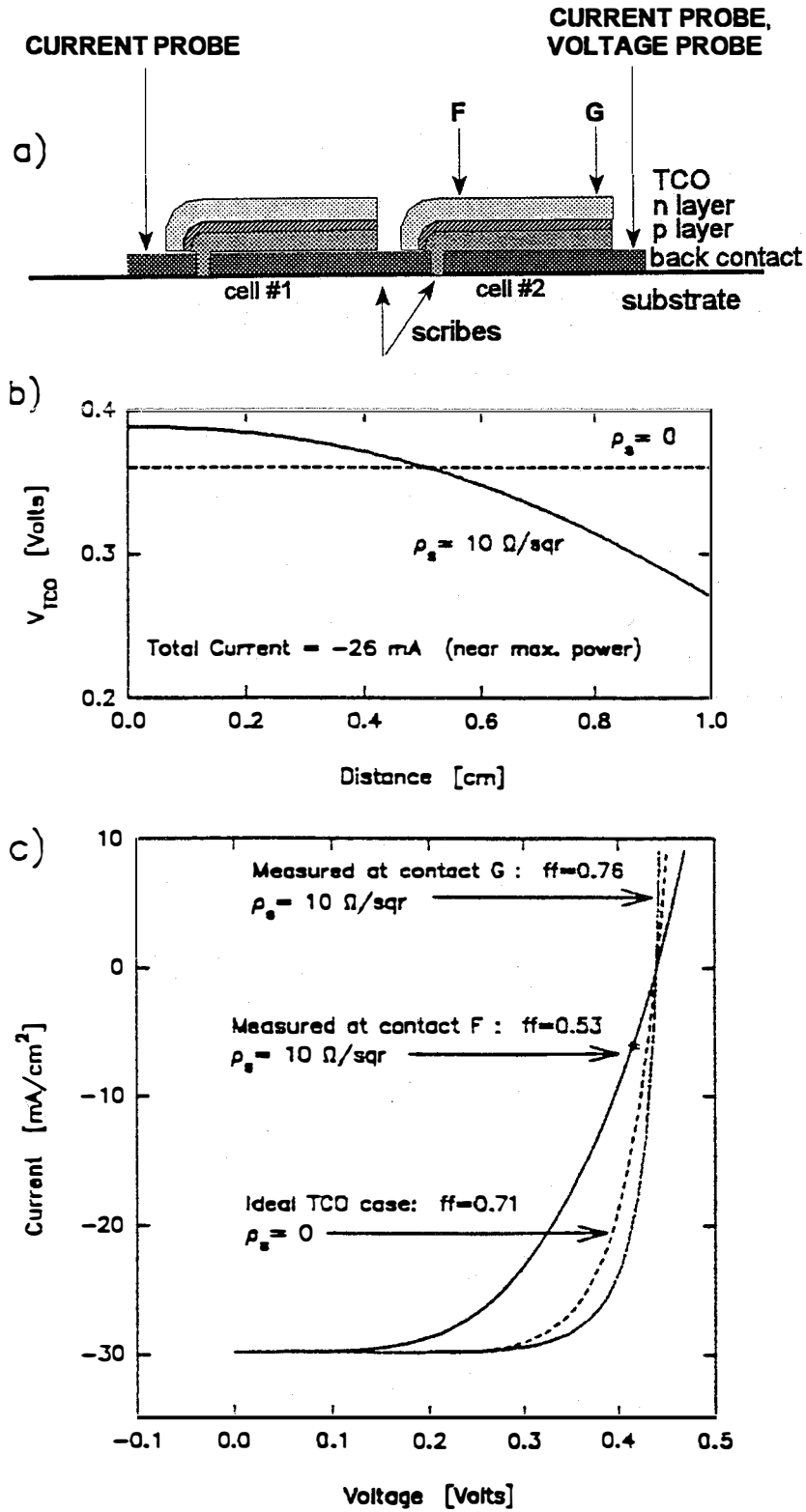


Figure 20. (a) Voltage-probe placement options and their consequences for (b) apparent maximum-power voltage and (c) apparent fill factor.

F, or at the interconnect between cells, gives the correct answer with the lower fill factor. The major change in voltage between G (distance = 0) and F (distance = 1 cm) is shown in Fig. 20b, again assuming a  $10 \Omega/\text{sqr}$  contact. The maximum power voltage at G, and the apparent fill factor with the probe placed at G, is in fact larger than that for an ideal, or zero resistance, conductor.

Several other features of module analysis, including (1) the failure of the linear series-resistance approximation, (2) the separation of photocurrent and shunt-resistance differences among cells in an encapsulated module by variation in chopped-light frequency, (3) the effect of forward bias on laser-scan measurements, and (4) the serious difficulties in interpreting laser scans of modules when bias light is used, were covered in the 1995 Annual report and will not be repeated here.

## RECOMMENDATIONS

The general recommendation is for a continuation and strengthening of the cooperative spirit among the laboratories fabricating and analyzing polycrystalline thin-film cells and modules. The teaming process initiated by NREL is an excellent strategy to promote the exchange of both ideas and specific results. A logical next step is to investigate ways to extend the teaming concept to the international community.

A second and more specific recommendation is to pin down the role of sodium, and perhaps other impurities, on CIS and CIGS junction quality. A related recommendation is to credibly sort out the roles of an indium-rich surface layer, carrier densities in the junction region, and band offsets between layers.

A third recommendation is a more aggressive attack on the junction limitations of CdTe cells. Maximum CdTe efficiency has not increased for nearly five years, and the physical model of the material is less mature than that of CI(G)S. Particularly since gallium can increase the CIS bandgap without an obvious downside, the question of whether CdTe junction quality has reached its practical limit is becoming an important question.

# COMMUNICATIONS

## Publications

- (1) J.E. Granata, J.R. Sites, G. Contreau-Puente, and A.D. Compaan, "Effect of CdS Thickness on CdS/CdTe Quantum Efficiency," *IEEE PVSC* **25** 853 (1996).
- (2) I.L. Eisgruber, "Thin-Film Module Measurement Artifacts," *IEEE PVSC* **25**, 829 (1996).
- (3) J.R. Tuttle, T.A. Barends, J. Keane, K.R. Ramanathan, J.E. Granata, R.N. Bhattacharya, H. Wiener, M.A. Contraras, and R. Noufi, "Investigations into Alternative Substrate, Absorber, and Buffer Layer Processing for Cu(In,Ga)Se<sub>2</sub>-Based Solar Cells," *IEEE PVSC* **25**, 797 (1996).
- (4) B. M. Basol, V.K. Kapur, A. Halini, C.R. Leidholm, J. Sharp, J.R. Sites, A. Swartzlander, R. Matson, and H. Ullal, "Cu(In,Ga)Se<sub>2</sub> Thin Films and Solar Cells Prepared by Selenization of Metallic Precursors," *J. Vac. Sci. Technol.* **A14**, 2251 (1996).
- (5) J.E. Granata, J.R. Sites, and J.R. Tuttle "Sodium Dependence of Cu(In,Ga) Se<sub>2</sub> Junction Electronics," *AIP Conf. Series*, **394**, 621 (1996)

## Presentations

CSM Colloquium	Golden	Sites	February 1996
PVSC Tutorial	Washington	Sites	May 1996
PVSC Oral Paper	Washington	Eisgruber	May 1996
Univ. Florida Colloquium	Gainesville	Sites	October 1996

## Graduate Degrees

- (1) Ingrid Eisgruber, (May 1996), Ph.D., Thesis: "Role of Nonuniformity in Thin-Film Polycrystalline Module Characterization."
- (2) Brendon Murphy, (August 1996), M.S. Coursework/Project Degree
- (3) Karl Schmidt, (August 1996), M.S. Coursework/Project Degree



## Reports

<u>Date</u>	<u>To</u>	<u>Done By</u>	<u>Topic</u>
1/22/96	CdTe Team	Granata/Sites	Thin CdS
2/23/96	CIS Guidance Team	Sites	Progress Report
5/15/96	CdTe Team	Granata/Sites	Thin CdS
7/17/96	GPI/Kester	Sites	Superstrate/TCD/Window Optics
8/5/96	Solarex/Kessler	Schmidt	High- $\rho$ ZnO
10/14/96	ISET/Basol	Sites	CIS Characterization
11/18/96	CdTe Team	Sites/Hiltner	Thin CdS
11/29/96	Emery/NREL NREL/Bhattacharya	Sites	High-Efficiency GPI Cell
12/13/96	Several Groups	Sites/Granata	High-Efficiency NREL-CIGS
12/17/96	ISET/Basol	Sites	CIS Characterization

# REPORT DOCUMENTATION PAGE

*Form Approved*  
OMB NO. 0704-0188

Public reporting burden for this collection of information is estimated to average 1 hour per response, including the time for reviewing instructions, searching existing data sources, gathering and maintaining the data needed, and completing and reviewing the collection of information. Send comments regarding this burden estimate or any other aspect of this collection of information, including suggestions for reducing this burden, to Washington Headquarters Services, Directorate for Information Operations and Reports, 1215 Jefferson Davis Highway, Suite 1204, Arlington, VA 22202-4302, and to the Office of Management and Budget, Paperwork Reduction Project (0704-0188), Washington, DC 20503.

1. AGENCY USE ONLY (Leave blank)	2. REPORT DATE October 1997	3. REPORT TYPE AND DATES COVERED Annual Subcontract Report, 6 December 1995 - 5 December 1996	
4. TITLE AND SUBTITLE  Device Physics of Thin-Film Polycrystalline Cells and Modules, Annual Subcontract Report, 6 December 1995 - 5 December 1996		5. FUNDING NUMBERS  C: XAX-4-14000-01 TA: PV704401	
6. AUTHOR(S)  J.R. Sites		8. PERFORMING ORGANIZATION REPORT NUMBER	
7. PERFORMING ORGANIZATION NAME(S) AND ADDRESS(ES)  Department of Physics Colorado State University Fort Collins, CO 80523-1875		10. SPONSORING/MONITORING AGENCY REPORT NUMBER  SR-520-23589	
9. SPONSORING/MONITORING AGENCY NAME(S) AND ADDRESS(ES)  National Renewable Energy Laboratory 1617 Cole Blvd. Golden, CO 80401-3393		11. SUPPLEMENTARY NOTES  NREL Technical Monitor: B. von Roedern	
12a. DISTRIBUTION/AVAILABILITY STATEMENT		12b. DISTRIBUTION CODE  UC-1263	
13. ABSTRACT ( <i>Maximum 200 words</i> ) During 1996, a number of projects were carried out at Colorado State University (CSU) on Cu(In,Ga)Se <sub>2</sub> (CIGS) and CdTe solar cells and small modules. CSU participated directly in the deposition of CIGS at NREL for the first time. Five separate substrates were used, and sodium was both deliberately introduced and deliberately blocked from exiting soda-lime substrates. In general, sodium in the CIGS led to better junction properties and higher efficiency. In other CIGS measurements, CSU showed that electrodeposited absorber material made at NREL produced competitive cells. Voltages, normalized to bandgap, were about 50 mV less than the best evaporated CIGS cells. CSU also showed, in collaboration with Solarex, that the existence of a high-resistivity ZnO layer is probably not critical for cells with relatively thick CdS window layers. In collaboration with seven CdTe fabrication laboratories, CSU measured the effect of CdS thickness on cell parameters. Although voltage and fill-factor generally degrade for CdS thickness below 100 nm, the exceptions suggest that with at least some fabrication techniques, CdS thickness can be reduced to the point that high quantum efficiency in the blue and a good diode junction are not mutually exclusive. A number of artifacts were investigated that appear in module measurement and analysis, but that are generally negligible for small test cells. These include effects due to module-cell geometry and misleading conclusions from selective illumination experiments. NREL data from the highest-efficiency CIGS and CdTe cells were analyzed to provide direct comparisons of different fabrication techniques. The three commonly used NREL deposition systems have produced CIGS cells with very similar junction properties. Similarly, after adjustment for bandgap, the best South Florida junctions from several years ago are remarkably similar to those produced by Golden Photon in 1996. CSU continues to play a significant role in both the CIGS Thin-Film and the CdTe projects summarized above.			
14. SUBJECT TERMS  photovoltaics ; device physics ; thin-film polycrystalline ; CIGS ; CdTe ; fabrication techniques		15. NUMBER OF PAGES 4 36	
17. SECURITY CLASSIFICATION OF REPORT Unclassified		16. PRICE CODE	
18. SECURITY CLASSIFICATION OF THIS PAGE Unclassified	19. SECURITY CLASSIFICATION OF ABSTRACT Unclassified	20. LIMITATION OF ABSTRACT  UL	